

引用格式: SHANG Chunlei, WANG Shi, LU Chengzhen, et al. Polarization State Variation Induced by the Circularly Polarized Light Scattering in LiNbO<sub>3</sub>:Fe Crystal (Invited)[J]. Acta Photonica Sinica, 2022, 51(1):0151113  
尚春雷,王石,卢城臻,等. LiNbO<sub>3</sub>:Fe 晶体中圆偏振光散射引起的偏振态变化(特邀)[J]. 光子学报, 2022, 51(1):0151113

# LiNbO<sub>3</sub>:Fe 晶体中圆偏振光散射引起的偏振态变化(特邀)

尚春雷,王石,卢城臻,梁春豪,高垣梅,蔡阳健,温增润

(山东师范大学 物理与电子科学学院 山东省光学与光子器件技术重点实验室 山东省光场调控工程技术研究中心, 济南 250358)

**摘 要:**报道了 LiNbO<sub>3</sub>:Fe 晶体内光致散射过程中偏振态的变化。将圆偏振光聚焦成极细的光片,并将其照射在 *c* 轴沿竖直方向放置的晶体上,研究了不同入射角时的光散射现象。在散射光从产生到达到稳态的数十分钟内,散射光主要在平行于 *c* 轴的方向上产生,同时在平行于光片的方向上存在分量,散射光产生速度随入射角的增大而减小。进一步观察表明,圆偏振光通过晶体后变成普通椭圆偏振光,不同入射角下出射光椭圆度也不同。结合晶体内部形成的噪声光栅,建立了圆偏振光的散射模型,并计算分析了偏振态变化的原因和机理。这一发现提出了一种利用光折变晶体的光致散射特性产生椭圆偏振光的方法,在基于光折变材料的光存储、光子晶格等方面有应用价值。

**关键词:**非线性光学;偏振;光折变晶体;光散射;光学存储

中图分类号:O734+.1

文献标识码:A

doi:10.3788/gzxb20225101.0151113

## 0 Introduction

The lithium niobate (LiNbO<sub>3</sub>) crystal is a negative uniaxial crystal ( $n_o > n_e$ ). BAUMAN A was the first to use the Czochralski technology to grow large-volume lithium niobate crystals in 1965. Since then, the properties of lithium niobate crystals have been widely studied and the crystals have been used for various applications<sup>[1]</sup>. In 1966, ASHKIN A et al<sup>[2]</sup> used LiNbO<sub>3</sub> and LiTaO<sub>3</sub> crystals to perform frequency doubling experiments and found that the refractive index of the irradiated region changed, namely, "optical damage". This kind of damage can be eliminated by high temperature heating. To distinguish it from permanent damage, this effect is referred to as photoinduced refractive index change or photorefractive effect which has been widely used in optical information storage<sup>[3-4]</sup>.

As a photorefractive material, the LiNbO<sub>3</sub> crystals have a variety of intrinsic defects<sup>[5]</sup>. When light enters the crystal, the intrinsic defects scatter the incident light. The scattered light interferes with the incident light, creating a grating structure inside the crystal<sup>[6]</sup> which is regarded as noise grating. The incident light transmits part of the energy to the scattered light through diffraction by the noise grating. As a result, the scattered light

**Foundation item:** National Key Research and Development Program of China (No. 2019YFA0705000), the National Natural Science Foundation of China (Nos. 91950104, 11525418, 91750201, 11974218, 11947239), the Innovation Group of Jinan (No. 2018GXRC010), the China Postdoctoral Science Foundation (No. 2019M662424)

**First author:** SHANG Chunlei (1997—), male, M.S. degree candidate, mainly focuses on nonlinear optics and photonic lattice. Email: shangchunlei@foxmail.com

**Supervisor:** GAO Yuanmei (1979—), female, professor, Ph.D. degree, mainly focuses on light manipulations, photonic lattice and optical tweezers. Email: gaoyuanmei@sdu.edu.cn

**Contact author:** CAI Yangjian (1977—), male, professor, Ph.D. degree, mainly focuses on light manipulations, optical transmission and atmospheric optics. Email: yangjiancai@suda.edu.cn

WEN Zengrun (1990—), male, lecturer, Ph.D. degree, mainly focuses on photonic lattice and laser technology. Email: wenzengrun@163.com

**Received:** Jul.19, 2021; **Accepted:** Aug.25, 2021

<http://www.photon.ac.cn>

gradually increases until it is stable. This phenomenon of light amplification, caused by the photorefractive effect, is called light-induced scattering<sup>[7]</sup>. The in-depth study of LiNbO<sub>3</sub> crystals resulted in the findings that the photorefractive effect of pure LiNbO<sub>3</sub> crystals is weak and that doping by certain metal ions can improve its photorefractive performance<sup>[8-9]</sup>. For example, in iron-doped LiNbO<sub>3</sub> crystals, the valence states of Fe<sup>2+</sup> and Fe<sup>3+</sup> ions are mutually transformed, which supports the "excitation-capture-re-excitation-re-capture" process of charge carriers, thereby enhancing the photorefractive effect of the crystal<sup>[10]</sup>.

In recent years, the light-induced scattering phenomena of photorefractive crystals have been extensively studied<sup>[11-23]</sup>. LIN Rong et al<sup>[24-26]</sup> studied the modulation instability and its influencing factors in LiNbO<sub>3</sub>:Fe crystals. ZHANG Yan and GAO Yuanmei et al<sup>[27-28]</sup> observed the scattering phenomenon of a focused beam incident on the LiNbO<sub>3</sub>:Fe crystal and found that the scattered light grew mainly along the direction of the incident beam. LU Chengzhen et al.<sup>[29]</sup> studied the scattering phenomena of e-light and o-light and their Energy Transfer Efficiency (ETE) and found that the ETE of o-light is higher than that of e-light. Since a single component of linearly polarized light is used for the incident, no variation of the polarization state of the outgoing light is observed. However, considering the difference in ETE between o-light and e-light, one has reason to guess that when another kind of light is incident, what's different from the outgoing light? According to our investigation, there is no research on this aspect at present.

In this work, we studied multiple groups of light-induced scattering phenomena in iron-doped LiNbO<sub>3</sub> crystal with different incident directions of circularly polarized light. After the scattered light was stabilized, we observed the noise grating in the crystal. Then, the polarization state of the light emitted after the crystal was checked by the light energy measurement along two orthogonal axes in the transverse direction. Simultaneously, the ellipticity of the light was calculated.

## 1 Experimental setup

The apparatus shown in Fig.1(a) is used to observe the scattering phenomena of the LiNbO<sub>3</sub>:Fe crystal (0.03 wt% Fe, 10 mm × 5 mm × 10 mm). The *c*-axis of the crystal is along the *y*-direction. The laser1 outputs linearly polarized light polarized in the vertical direction, with a power of 200 mW and a wavelength of 532 nm. A Quarter Wave Plate (QWP), a Spatial Filter (SF), a convex lens (L<sub>1</sub>) and a cylindrical lens (L<sub>4</sub>) form a beam shaping system. The beam passes through the shaping system to become a band-shaped beam (light sheet), which then irradiates the crystal. The far-field scattering image appears on the Optical Screen (OS). When the collimated parallel light is irradiated onto the cylindrical lens, due to the unidirectional focusing character of the cylindrical lens, the light beam can be focused to be a sheet in a certain direction at the focal point, then expanding in this direction. That's why the light sheet on the screen rotates 90° relative to the light sheet incident on the crystal. The cylindrical lens is rotated so that the angles (between the incident light sheet

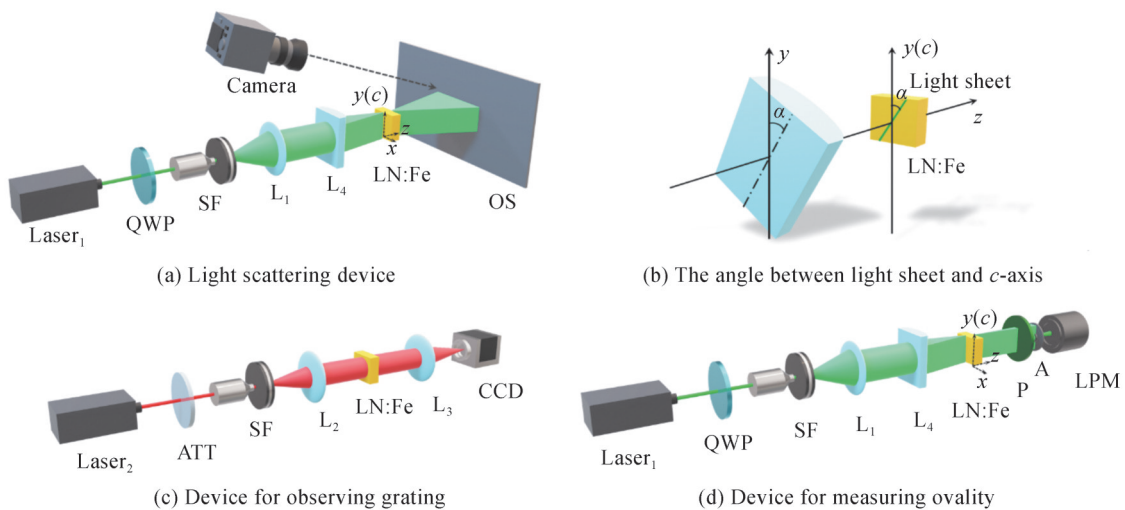


Fig.1 Experimental setup and light path diagram

and the  $c$ -axis of the crystal) are altered as  $\alpha=0^\circ$ ,  $30^\circ$ ,  $45^\circ$ ,  $60^\circ$ , and  $90^\circ$  relative to the  $y$ -axis, as shown in Fig.1(b). The scattering image was recorded using a camera (Canon EOS 70D).

The device shown in Fig.1(c) was used to observe the noise grating in the LiNbO<sub>3</sub>:Fe crystal. The laser passing through the attenuator (ATT) passes through the SF and the lens ( $L_2$ ), irradiates on the crystal, and then images through the lens ( $L_3$ ). The raster information is captured by the Charge Coupled Device (CCD) and displayed on the computer screen. The laser 2 outputs linearly polarized light polarized in the vertical direction, with a power of 50 mW and a wavelength of 632 nm. Laser 1 has high coherence and will produce more noise when used as readout light to disturb the original grating pattern. Therefore, laser 2 with low coherence and low power is selected to avoid disturbing the grating pattern.

The device shown in Fig.1(d) is used to determine the polarization state of the light after passing through the crystal. The scattered light passes through the polarizer (P) and the aperture (A, with a diameter of 4 mm) in turn and is received by the Laser Power Meter (LPM). The aim is achieved by rotating the polarizer and recording the maximum power ( $P_{\max}$ ) and the minimum power ( $P_{\min}$ ) by the LPM. The intensity of the scattered light located in the scattering areas on both sides is much less than the central light intensity. The comparison between  $P_{\max}$  and  $P_{\min}$  is not obvious, and the measurement error is large. Therefore, the polarization state of the scattered light in the central area is measured. The ellipticity is usually expressed by the ratio of the semi-major axis to the semi-minor axis, so the ellipticity of the beam can be calculated by the following formula

$$\rho = \frac{A_{\min}}{A_{\max}} = \sqrt{\frac{I_{\min}}{I_{\max}}} = \sqrt{\frac{P_{\min}}{P_{\max}}} \quad (1)$$

where  $A_{\min}$  and  $A_{\max}$  are the amplitudes of semi-minor axis and semi-major axis respectively, and  $I_{\min}$  and  $I_{\max}$  are the corresponding light intensity.

## 2 Experimental results

### 2.1 Light scattering results under different configurations

The light-induced scattering phenomenon of LiNbO<sub>3</sub>:Fe crystal has a strong regularity. An image is taken every 5 s and choose five of them for each polarization angle. The light scattering patterns at five angles are shown in Fig.2, where  $c$  represents the  $c$ -axis and  $f$  represents the light sheet direction. The light distribution on the screen showed that the scattered light was rapidly generated in a few minutes and the scattered light was not continuous, but consists of closely spaced filaments paralleling to the light sheet, and the filaments extend with the growth of the scattered light, as shown in the white dashed box in Fig.2(a). The growth of the scattered light is not only perpendicular to the light sheet beam but also presents along the light sheet beam. As shown in Fig.2(a)~(e), it is clear that the length of the light sheet on the screen increases with the angle, indicating that the incident light energy has been transmitted in two perpendicular directions. However, the light scattering laws under the five configurations are not completely identical. When  $\alpha=0$  is set, the scattered light grows rapidly to both sides with the incident beam as the center, and the growth direction is parallel to the  $c$ -axis of the crystal, that is, parallel to the incident light sheet, as shown in Fig.2(a). The angle between the strip beam and the crystal  $c$ -axis was adjusted to  $30^\circ$ ,  $45^\circ$ , and  $60^\circ$  respectively, and the light scattering results are shown in Fig.2(b), (c) and (d). The scattered light exists not only in the direction parallel to the light sheet but also in the direction parallel to the  $c$ -axis of the crystal. Moreover, with the increase of angle  $\alpha$ , the scattered light component perpendicular to the light sheet also increases. When  $\alpha$  is  $90^\circ$ , the scattered light mainly intensifies along the direction parallel to the  $c$ -axis, that is, perpendicular to the direction of the light sheet. But there is a component in the direction perpendicular to the light sheet. When  $\alpha$  is set to 0 or  $90^\circ$ , the scattering pattern is axisymmetric, while at other angles, the scattering pattern is not axisymmetric. This is because the scattering component extending along the  $f$ -direction is affected by the nonlinearity of the  $c$ -axis direction, and the whole scattering pattern extends along the positive and negative  $c$ -axis direction, resulting in the non-axisymmetric diffraction pattern. In addition, the speed of scattered light growth is different for various angles  $\alpha$ . The time taken to reach a steady state in Fig.2(a), (b), (c), (d), and (e) is 10 min, 20 min, 30 min, 50 min, and 70 min, respectively. The scattering law can be obtained: the light scattering is mainly concentrated in the direction parallel to the  $c$ -axis. When there is a certain angle between the incident light direction and the  $c$ -axis direction,

there is a component of the scattered light in the direction perpendicular to the light sheet. The smaller the angle between the incident light sheet and  $c$ -axis, the faster it reaches the steady state.

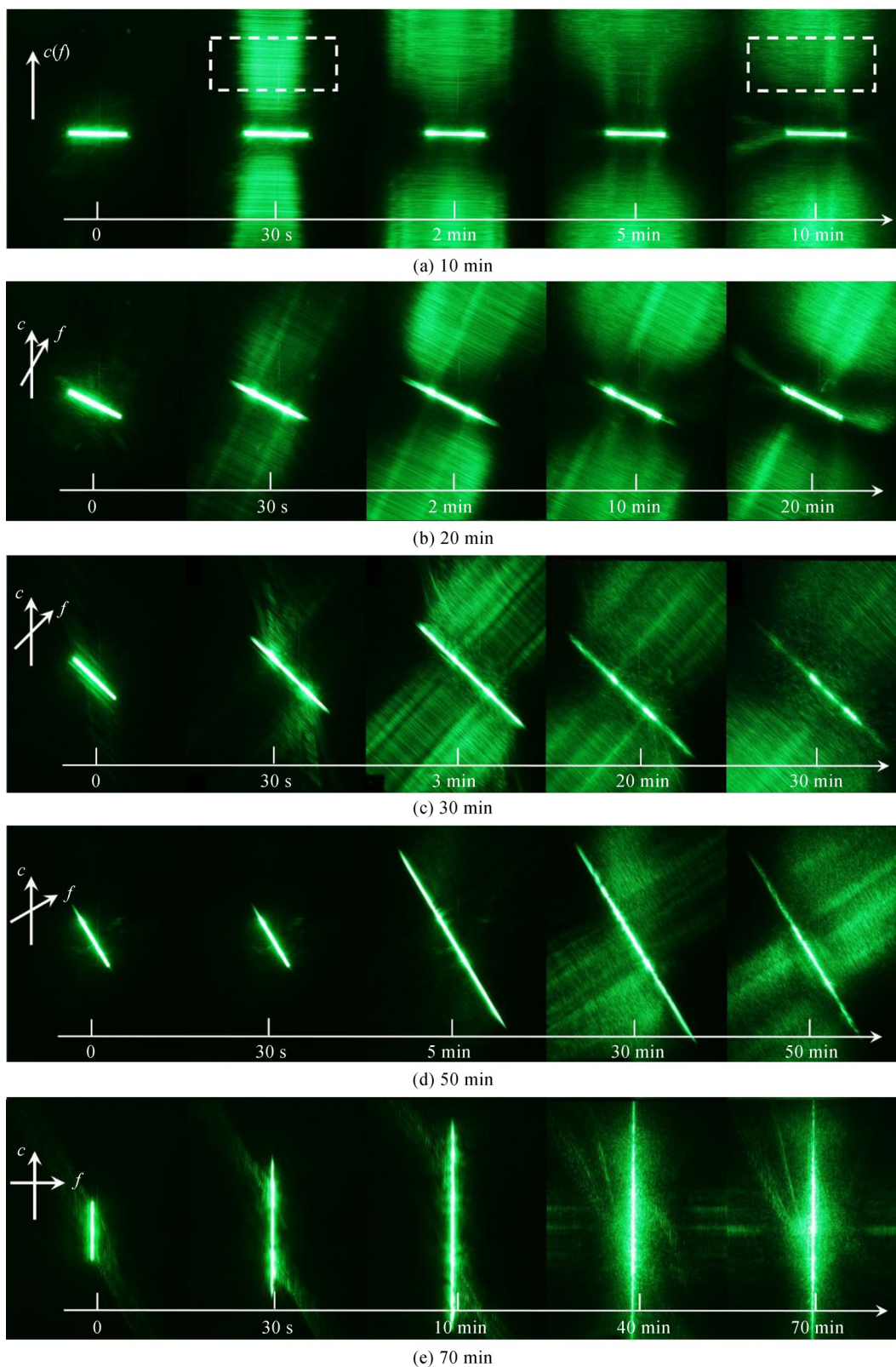


Fig.2 Scattered light at  $\alpha=0, 30^\circ, 45^\circ, 60^\circ$  and  $90^\circ$  respectively

After the scattered light reaches the steady state, the noise grating inside the crystal is observed using the device of Fig.1 (c). The  $30^\circ, 45^\circ, 60^\circ,$  and  $90^\circ$  noise gratings are the composition of two chirped gratings, as



shown in Fig. 3 (a) ~ (d). It can be seen that the grating appears as dense straight stripes, and the stripes direction is the same as the growth direction of the scattered light. However, the gratings are not uniform, and the densities of the gratings increase from the middle to the sides. The reason is that the focused beam has “self-defocusing” in the crystal. It is necessary to observe the distribution of noise grating for the next study of the mechanism of light-induced scattering.

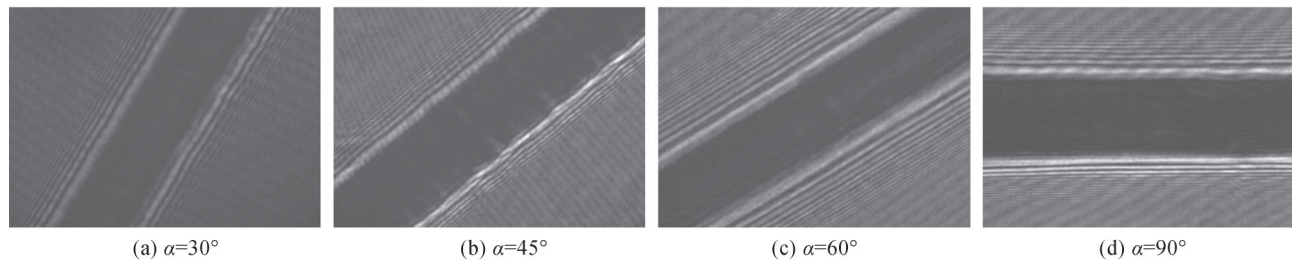


Fig.3 Noise grating in the crystal at different incident angles

## 2.2 Measurement of the polarization state of scattered light

The polarization state of the output light is measured by the device shown in Fig.1(d) and characterized by ellipticity. Through Eq. (1), the polarization states at the center of the outgoing light at different incident angles are calculated. It is found that the circularly polarized light becomes elliptically polarized light after passing through the crystal. The ellipticities are measured several times and the averages are shown in Fig.4. When the incident angle  $\alpha=30^\circ$  or  $45^\circ$ , the emitted light is close to the circularly polarized light, and at other incident angles, the emitted light is elliptically polarized light significantly.

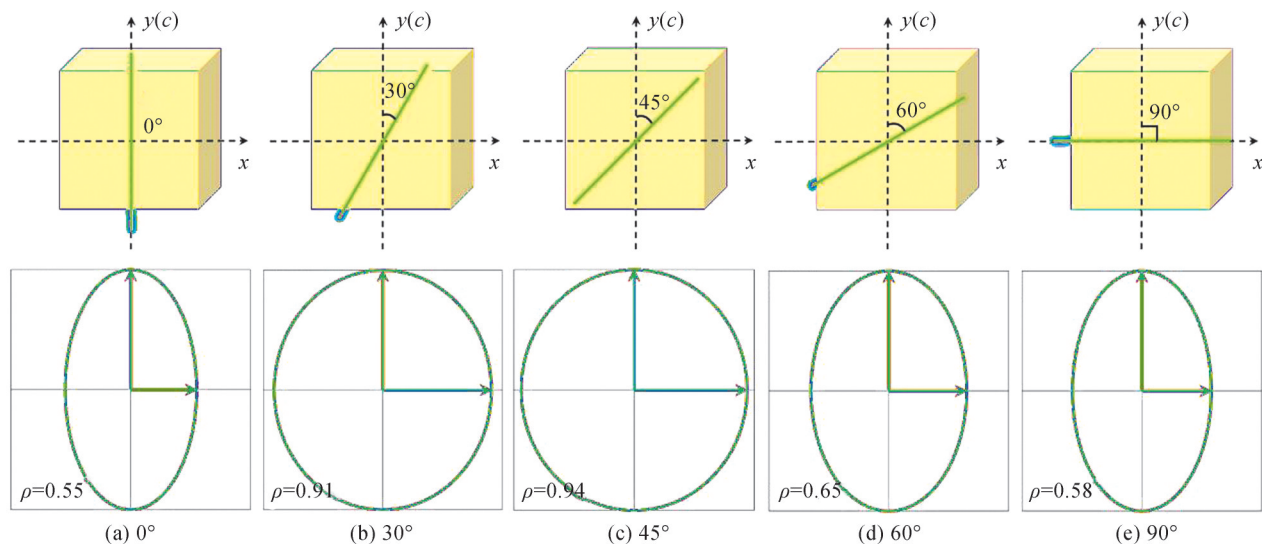


Fig.4 Polarization state of outgoing light at different incident angles

## 3 Discussion

### 3.1 Light crawling model and scattering mechanism

When the beam irradiates the LiNbO<sub>3</sub>: Fe crystal, light scattering of nearly  $90^\circ$  was observed, and light scattering crawling along the crystal optical axis direction in the crystal was detected as well<sup>[30]</sup>, as shown in Fig.5. This experiment proved that this type of crawling light scattering causes energy dissipation. The energy of the scattered light leaks from the crystal during the crawling process is the energy source of the light scattered at nearly  $90^\circ$ . Taking  $\alpha=90^\circ$  as an example, Fig.5(a), (b) show the angle of the incident of the light sheet, and Fig.5(c) shows the light crawling model, and the scattered light on the optical screen is shown in Fig.5(d). When the crystal is irradiated, only the forward-scattered light with a wide scattering angle can travel a long

distance in the irradiation area, thus passing through the noise grating and obtaining more energy from the incident light. Scattered light with a wide reflection angle may pass through multiple reflections in the irradiated area and obtain effective amplification. The light with a small scattering angle directly passes through the crystal without grating, which makes little contribution to the scattered light. During crawling, scattering also results in local refractive index changes in the crystal, which in turn causes the scattered light to be produced continuously. Light and dark parallel stripes can be seen in the light crawling area and are stored in the crystal, as shown in Fig.3. This qualitatively explains why the scattered light is composed of closely arranged filaments and the formation process of the chirped grating.

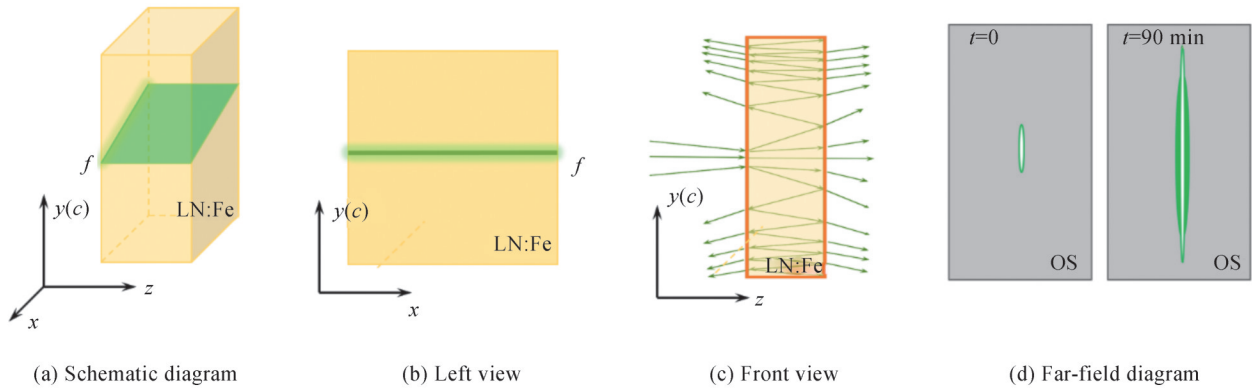


Fig.5 Light crawling and light scattering model

The incident light beam forms a grating in the crystal as shown in Fig.3, and the grating expands to both sides with the light beam as the center. The grating diffracts continuous light, i. e. light-induced self-diffraction<sup>[31-32]</sup>. Light-induced light scattering and light-induced self-diffraction are competing processes. When the direction of the light stripe is the same as the direction of the crystal *c*-axis, light-induced self-diffraction and light-induced light scattering occur at the same time. The process by which incident light transfers energy. When the included angle is 30°, 45°, or 60°, it takes a certain time (time for light scattering to reach saturation) to form the phase grating. At the beginning, the phenomenon of "light overflow" occurs in the direction perpendicular to the beam, that is, at this time, light-induced self-diffraction dominates, and more energy is obtained from the incident light. However, as light-induced light scattering gradually dominates the competition, the energy of incident light is eventually transferred to light-induced light scattering. Therefore, light-induced light scattering still plays a major role in the scattering effect. When the included angle is 90°, the photorefractive effect is the weakest, the scattering phenomenon is not easy to observe, and the energy transferred from the incident light is the least. In addition, in the sub-beam passing region, electrons are excited to form electron-hole pairs. Electrons and holes are two types of scattering sources for incident light. Under continuous illumination, when the concentration of the scattering sources in the illumination area is balanced, the light scattering reaches a steady state.

### 3.2 Analysis of polarization state change

We establish the scattering model of the crystal to the circularly polarized light to analyze the polarization state of the scattered light, as shown in Fig.6. The circularly polarized light propagating along the *z*-axis is focused by a cylindrical lens into a narrow light sheet *f*. the angles between the scattered light and the *x*-axis and *y*-axis are  $\varphi$  and  $\theta$ , respectively. The electric field vector expression of circularly polarized light is

$$\mathbf{E} = A_0 [\cos(\omega t) \mathbf{e}_x \mp \sin(\omega t) \mathbf{e}_y] \quad (2)$$

where  $\mathbf{E}$  is the electric field vector,  $A_0$  is the amplitude of the component in the *x* or *y* direction, and  $\mathbf{e}_x$ ,  $\mathbf{e}_y$  are the unit vectors along the *x* and *y*-axis. Let the electric field components of the emitted light in *x*, *y*-axis be  $E_x$ ,  $E_y$ , then

$$\begin{cases} E_x = \tau_x A_0 \cos(\omega t) \sin \varphi \\ E_y = \tau_y A_0 \cos(\omega t + \delta) \sin \theta \end{cases} \quad (3)$$

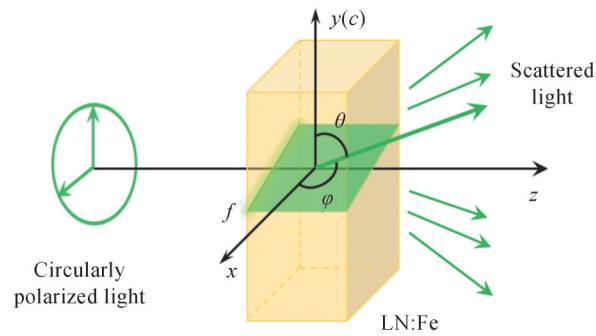


Fig.6 The model of polarization state change of scattered light

$\delta$  is the phase difference between e-light and o-light caused by crystal. Let

$$\begin{cases} \tau_x \sin \varphi A_0 = A_x \\ \tau_y \sin \theta A_0 = A_y \end{cases} \quad (4)$$

then

$$\begin{cases} E_x = A_x \cos(\omega t) \\ E_y = A_y \cos(\omega t + \delta) \end{cases} \quad (5)$$

assuming  $A_x < A_y$ , the ellipticity of scattered light can be expressed as

$$\rho = \frac{A_x}{A_y} = \frac{\tau_x \sin \varphi}{\tau_y \sin \theta} \quad (6)$$

It can be seen from Eq. (6) that the ellipticity of scattered light is related to the transmission coefficient  $\tau$  and azimuth angle, and the left-handed or right-handed polarization state is also related to the phase difference  $\delta$ . Because of the anisotropy and photorefractive effect of crystal, it is difficult to calculate its value, but qualitative analysis can be done. The polarization state transition effect of LiNbO<sub>3</sub>:Fe crystal can be used to obtain elliptically polarized light from circularly polarized light.

## 4 Conclusion

In summary, the scattering phenomena generated by circularly polarized light irradiating a LiNbO<sub>3</sub>:Fe crystal was investigated. The scattered light mainly grows in the direction parallel to the  $c$ -axis and has a component in the direction parallel to the light sheet, and the growth speed of the scattered light decreases with the increase of the incident angle  $\alpha$ . Moreover, circularly polarized light degrades into ordinary elliptically polarized light after passing through the crystal. We use the light crawling model to analyze the generation mechanism of scattered light and noise grating, calculate the ellipticity of the outgoing light, and analyze the cause of polarization state degradation. We establish the scattering model of circularly polarized light and analyze the reason why circularly polarized light degenerates into elliptically polarized light in this process. In addition, this research inspired us to use the light-induced scattering properties of photorefractive crystals to generate elliptically polarized light. The light-induced light-scattering enhances the system noise to a certain extent. This noise will persist and weaken the incident light energy, which causes issues for the applications of photorefractive materials. This work provides a reference for elliptically polarized light generation, optical storage and photonic lattice research, thus leading to the improvement of photorefractive material applications and technologies.

## References

- [1] HOLSTEIN W L. Etching study of ferroelectric microdomains in LiNbO<sub>3</sub> and MgO:LiNbO<sub>3</sub>[J]. Journal of Crystal Growth, 1997, 171(3-4): 477-484.
- [2] ASHKIN A, BOYD G D, DZIEDZIC J M, et al. Optically-induced refractive index inhomogeneities in LiNbO<sub>3</sub> and LiTaO<sub>3</sub>[J]. Applied Physics Letters, 1966, 9(1): 72-74.
- [3] CHEN F S, LAMACCHIA J T, FRASER D B. Holographic storage in lithium niobate[J]. Applied Physics Letters, 1968, 13(7): 223-225.
- [4] CHEN F S. Optically induced change of refractive indices in LiNbO<sub>3</sub> and LiTaO<sub>3</sub>[J]. Journal of Applied Physics, 1969, 40

- (8): 3389-3396.
- [5] IYI N, KITAMURA K, IZUMI F, et al. Comparative study of defect structures in lithium niobate with different compositions[J]. Journal of Solid State Chemistry, 1992, 101(2): 340-352.
- [6] LIU J P, LEE H Y, YAU H F, et al. One-beam recording in a LiNbO<sub>3</sub> crystal[J]. Optics Letters, 2005, 30(3): 305-307.
- [7] DAI Cuixia, LIU Liren, LIU Dean. Photorefractive coherent scattering noise[J]. Laser & Optoelectronics Progress, 2005, 42(10): 14-17.
- [8] SAVCHENKOV A A, MATSKO A B, STREKALOV D, et al. Photorefractive effects in magnesium doped lithium niobate whispering gallery mode resonators[J]. Applied Physics Letters, 2006, 88(24): 241909.
- [9] YAN Wenbo, LI Yangxian, SHI Lihong, et al. Photochromic effect in LiNbO<sub>3</sub>:Fe:Co.[J]. Optics Express, 2007, 15(25): 17010-17018.
- [10] JERMANN F, OTTEN J. Light-induced charge transport in LiNbO<sub>3</sub>:Fe at high light intensities[J]. Journal of the Optical Society of America B, 1993, 10(11): 2085-2092.
- [11] ZHANG Guoquan, TIAN Guoyun, LIU Simin, et al. Noise amplification mechanism in LiNbO<sub>3</sub>:Fe crystal sheets[J]. Journal of the Optical Society of America B, 1997, 14(11): 2823-2830.
- [12] GUO Ru, PAN Shihong, ZHANG Guangyin. Steady state beam fanning in photorefractive crystals[J]. Acta Physica Sinica, 1996, 45(12): 2005-2009.
- [13] LIU Simin, ZHANG Guangyin, WU Yuanqing, et al. Observation of laser-induced self-diffraction from LiNbO<sub>3</sub>:Fe crystal[J]. Chinese Physics, 1988, 37(2): 268-273.
- [14] GUO Ru, LIU Simin, LING Zhenfang, et al. Symmetric beam fanning in photorefractive crystals with a local nonlinear response[J]. Acta Physica Sinica, 1997, 46(8): 138-142.
- [15] GAO Yuanmei, LIU Simin, ZHAO Hongge, et al. Light coupling in c-cut doped lithium niobate crystals[J]. Acta Physica Sinica, 2003, 52(5): 1162-1167.
- [16] GAO Yuanmei, LIU Simin, GUO Ru, et al. Light coupling in Y-cut doped lithium niobate crystals[J]. Acta Physica Sinica, 2004, 53(9): 2958-2963.
- [17] LIU Dean, LIU Liren, REN Liyong, et al. Material optimization for low scattering noise during nonvolatile holographic recording in doubly doped LiNbO<sub>3</sub> crystals[J]. Chinese Optics Letters, 2004, 2(11): 630-633.
- [18] BUSE K, DENZ C, KROLIKOWSKI W. Photorefractive materials, effects, and devices: introduction [J]. Applied Physics B, 2009, 95(3): 389-390.
- [19] MAXEIN D, BUECKERS J, HAERTLE D, et al. Photorefractive effects in LiNbO<sub>3</sub>:Fe crystals with femtosecond laser pulses [J]. Applied Physics B, 2009, 95(3): 399-405.
- [20] BERNERT C, HOPPE R, WITTEW F, et al. Ptychographic analysis of the photorefractive effect in LiNbO<sub>3</sub>:Fe[J]. Optics Express, 2017, 25(25): 31640-31650.
- [21] KAMBER N Y, XU Jingjun, MIKHA S M, et al. Threshold effect for photorefractive light-induced scattering and signal beam amplification in doped LiNbO<sub>3</sub> crystals [J]. Journal of Applied Physics, 2000, 87(6): 2684-2690.
- [22] KAMBER N Y, XU Jingjun, MIKHA S M, et al. Threshold effect of incident light intensity for the resistance against the photorefractive light-induced scattering in doped lithium niobate crystals[J]. Optics Communications, 2000, 176(1-3): 91-96.
- [23] KWON O P, JAZBINSEK M, GUENTER P, et al. Backward beam fanning in organic photorefractive devices [J]. Applied Physics Letters, 2006, 89(2): 021905.
- [24] RONG Lin, GAO Yuanmei. Observation of the modulation instability and frequency-doubling in self-defocusing crystal [J]. Physics Letters A, 2011, 375(36): 3228-3231.
- [25] RONG Lin, GAO Yuanmei. Observation of the modulation instability induced by both intrinsic noise and the amplitude mask with periodic lattices[J]. Optik, 2015, 126(19): 1757-1760.
- [26] RONG Lin, GAO Yuanmei. Factors that influence the modulation instability in self-defocusing photorefractive crystal[J]. Optics Communications, 2012, 285(10-11): 2724-2728.
- [27] ZHANG Yan, ZHAO Yuefeng, HAO Lina, et al. Special scattering in photorefractive crystal LiNbO<sub>3</sub>:Fe [J]. Acta Physica Sinica, 2017, 66(8): 141-146.
- [28] GAO Yuanmei, LV Jing, LIN Rong, et al. Special scattering of extraordinary light in Photorefractive LiNbO<sub>3</sub>:Fe crystal [J]. Optik, 2017, 149: 295-299.
- [29] LU Chengzhen, QI Xinyuan, CAI Yangjian, et al. Study of the scattered light with the strip beam incident to the LiNbO<sub>3</sub>:Fe crystal[J]. Optik, 2019, 181: 1163-1168.
- [30] LIU Simin, XU Jingjun, ZHANG Guangyin, et al. Light-climbing effect in LiNbO<sub>3</sub>:Fe crystal. [J]. Applied Optics, 1994, 33(6): 997-999.
- [31] ANGELSKY O V, BEKSHAEV A Y, MAKSIMYAK P P, et al. Self-diffraction of continuous laser radiation in a disperse medium with absorbing particles[J]. Optics Express, 2013, 21(7): 8922-8938.



- [32] ANGELSKY O V, BEKSHAEV A Y, MAKSIMYAK P P, et al. Self-action of continuous laser radiation and Pearcey diffraction in a water suspension with light-absorbing particles[J]. Optics Express, 2014, 22(3): 2267–2277.

## **Polarization State Variation Induced by the Circularly Polarized Light Scattering in LiNbO<sub>3</sub>:Fe Crystal (Invited)**

SHANG Chunlei, WANG Shi, LU Chengzhen, LIANG Chunhao, GAO Yuanmei,  
CAI Yangjian, WEN Zengrun

*(Center of Light Manipulations and Applications & Shandong Provincial Key Laboratory of Optics and Photonic  
Device, School of Physics and Electronics, Shandong Normal University, Jinan 250358, China)*

**Abstract:** Doped LiNbO<sub>3</sub> crystal is one kind of photorefractive mediums which are used for optical storage. When light passes through LiNbO<sub>3</sub> crystal, it will cause local refractive index change and form noise grating. The noise grating diffracts the incident light, transferring part of the light energy to the scattered light, namely, light-induced scattering. In recent years, the modulation instability, generation process and energy transfer efficiency of light scattering in LiNbO<sub>3</sub> crystals have been widely studied. Since a single component of linearly polarized light is used for the incident, no variation of the polarization state of the outgoing light is observed. However, considering the difference of energy transmission efficiency between o-light and e-light, it is reasonable to guess that the polarization state of the outgoing light may change when another light is incident. According to our investigation, there is no research in this field. In this work, the variation of the polarization state of LiNbO<sub>3</sub>:Fe crystal during the light-induced scattering process is reported. The circularly polarized light is focused into a thin light sheet and irradiated on the crystal with the *c*-axis along the vertical direction. The light scattering phenomenon at different incident angles is studied. In the tens of minutes from the generation of the scattered light to the steady state, the scattered light mainly grows in the direction parallel to the *c*-axis, and there is also a component in the direction parallel to the light sheet. The growth rate of scattered light decreases with the increase of the incident angle. Further observation manifests that the circularly polarized light becomes ordinary elliptically polarized light after passing through the crystal, and the ellipticity varies with the incident angle. Combined with the noise grating formed in the crystal, the scattering model of circularly polarized light is established, and the reason and mechanism of polarization state change are analyzed through calculation. Qualitative analysis shows that the ellipticity of scattered light is related to the transmission coefficient  $\tau$  and azimuth angle, and the left-handed or right-handed polarization state is also related to the phase difference  $\delta$  between o-light and e-light. This discovery proposes a method to generate elliptically polarized light using the light-induced light-scattering properties of photorefractive crystals, which can be applied to optical storage and photonic lattice based on photorefractive materials.

**Key words:** Nonlinear optics; Polarizations; Photorefractive crystals; Light scattering; Optical storage

**OCIS Codes:** 050.1590; 260.1180; 260.2130; 210.4810; 050.1590